APPLICATION OF MACHINE LEARNING FOR RADIO REFRACTIVITY PREDICTION ACROSS CLIMATIC ZONES IN WEST AFRICA

Abstract-This study explores the use of machine learning (ML) models to predict surface radio refractivity in diverse climatic zones across West Africa, focusing on five representative locations: Niamey, Bamako, Monrovia, Dakar, and Jos. Surface radio refractivity, a critical factor influencing radio wave propagation and wireless communication, was computed using key atmospheric parameters from the ERA5 reanalysis dataset. Three ML models; LightGBM, Random Forest, and Long Short-Term Memory (LSTM), were trained and optimized through grid search and early stopping to improve predictive accuracy. The study evaluates the models' performance across different climatic zones and seasons, identifying LightGBM as the most accurate overall followed by random forest while LSTM showed better performance in regions with high seasonal variability. This research highlights the potential of ML for enhancing radio refractivity prediction and provides insights into the most important atmospheric predictors for different regions in West Africa.

Keywords: Machine learning, Radio refractivity, Atmospheric prediction, ERA5, West Africa, LightGBM, Random Forest, LSTM

1. INTRODUCTION

Radio wave propagation is integral to modern communication systems, such as wireless networks, satellite communications, and radar systems. The propagation characteristics of radio waves are heavily influenced by atmospheric conditions, with radio refractivity playing a critical role in determining signal paths as shown in figure 1. Phenomena such as scattering, absorption, reflection, and refraction within the Earth's troposphere govern radio wave behaviour (Adeniji et al., 2021). The troposphere, spanning approximately 10 km at the poles and 17 km at the equator, directly impacts human activities (Hall, 1979). In regions like West Africa, characterized by diverse climatic zones, from arid regions in the north to humid tropical areas in the south, accurate prediction of surface refractivity is essential for optimizing radio frequency applications.

Traditional methods for predicting radio refractivity often rely on empirical models that may not adequately account for the complexities of atmospheric behavior. In recent years, machine learning (ML) techniques have emerged as powerful alternatives, offering the ability to model nonlinear relationships and capture intricate patterns within atmospheric data. The primary aim of this research is to explore and compare different machine learning models for predicting surface refractivity. The models analyzed in this study include LightGBM, Random Forest, and Long Short-Term Memory (LSTM). Each model was trained and optimized using data from ERA5 reanalysis, a widely used global atmospheric dataset. Through a comprehensive analysis that includes metrics such as Mean Absolute Error (MAE) and Mean Squared Error (MSE), this study seeks to provide insights into model performance across various locations; Niamey, Bamako, Monrovia, Darker, and Jos, and different seasonal conditions representing a broad spectrum of climatic zones. The

findings will contribute to a better understanding of how machine learning can enhance refractivity predictions and improve the reliability of wireless communication systems in challenging atmospheric environments.

Objectives

a) Compare the performance of machine learning models (LightGBM, Random Forest, LSTM) in predicting surface refractivity.
b) Identify the most effective model for predicting surface refractivity in different climatic zones and seasons.
c) Determine the most important predictors influencing refractivity in West Africa.

2. LITERATURE REVIEW

Machine learning models have shown promising results in meteorological applications such as temperature forecasting, humidity estimation, and rainfall prediction. These models excel at capturing complex non-linear relationships between atmospheric variables, which is critical in accurately predicting radio refractivity.

Several studies have applied ML techniques for atmospheric refractivity prediction in various regions. For instance, Kalansuriya et al. (2015) used Support Vector Machines (SVM) and Artificial Neural Networks (ANNs) to predict refractivity, another method, which is Downscaling techniques have been widely used to improve regional climate predictions, especially in diverse climatic zones like West Africa (Wilby & Dawson, 2013), noting substantial improvements in accuracy compared to traditional models. However, their work focused on relatively homogeneous climatic conditions, leaving a gap in understanding how ML models perform across varied climates such as those in West Africa. In addition, models like LSTM, which are well-suited for time-series data, have shown effectiveness in predicting atmospheric variables that exhibit seasonal variations

(Thies & Bendix, 2011). Yet, there remains limited research on applying these advanced ML models specifically for surface refractivity prediction in diverse climates. This paper aims to fill this gap by analyzing multiple ML models and their performance across West Africa's distinct climatic zones.

3. METHODOLOGY

3.1 Study Locations: This study focuses on five key locations across West Africa, selected to represent a diverse range of climatic conditions, as shown in **Table 1**. These regions exhibit significant variations in temperature, humidity, and seasonal patterns, all of which are expected to influence surface refractivity. Each of these locations represents a distinct climatic zone with unique atmospheric dynamics.

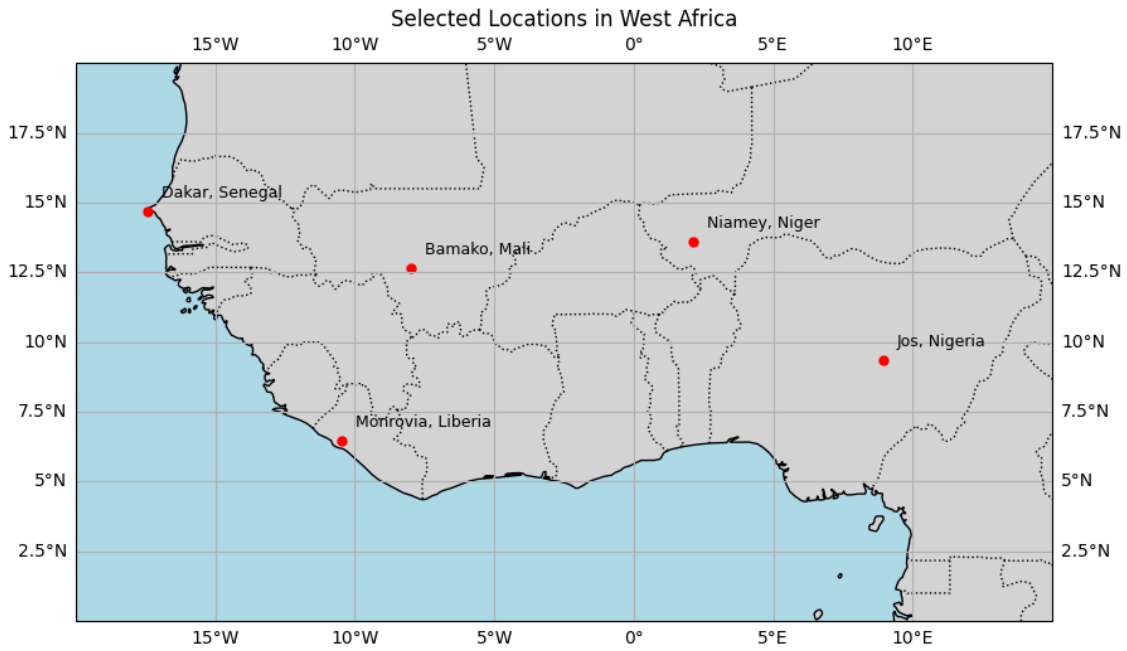

Figure 1: Map showing the selected study locations across West Africa, each representing distinct climatic zones.

Table 1: Selected study locations in West Africa

City	Country	Climate Zone
Niamey	Niger	Sahel

Bamako	Mali	Sudano-Sahelian
Monrovia	Liberia	Tropical Rainforest
Dakar	Senegal	Tropical Savanna
Jos	Nigeria	Tropical Wet and Dry

3.2 Data Collection and Preprocessing: Data for surface refractivity prediction were derived from the ***ERA5 reanalysis dataset*** provided by the European Centre for Medium-Range Weather Forecasts (ECMWF). ERA5 offers high-resolution global atmospheric data, including surface temperature, pressure, and relative humidity, critical inputs for calculating surface refractivity (Dee et al., 2011). The equation used for calculating surface refractivity (N) is given as: $$N = 77.6 \times \frac{P}{T} + 3.73 \times 10^5 \times \frac{e}{T^2}$$

Where:
- P is the atmospheric pressure (hPa)
- T is the temperature (K)
- e is the water vapor pressure (hPa)

Data preprocessing involved extracting relevant atmospheric parameters from ERA5, including surface temperature, pressure, and humidity, at a daily time resolution. The data was further aggregated to compute seasonal averages to analyze the performance of models across different seasons.

3.2.1. Atmospheric Predictors: In this study, four key atmospheric predictors were used to model surface refractivity:

a) **Potential Evaporation (m)**: This predictor represents the amount of water that could evaporate under given atmospheric conditions, contributing to variations in humidity, which directly affects radio refractivity. Higher evaporation rates typically reduce humidity and refractivity (Gentine et al., 2018).

b) **Surface Net Solar Radiation (Jm^{-2})**: Solar radiation influences surface temperature and atmospheric density, which are critical to refractivity. Increased solar radiation

heats the surface, altering the temperature profile and subsequently affecting refractivity levels (Wilby & Dawson, 2013).

c) **Wind Speed (ms^{-1})**: Wind speed plays a role in transporting heat and moisture across regions, influencing both temperature and humidity. Variations in wind speed can lead to localized changes in atmospheric refractivity (Bouma et al., 2021).

d) **Precipitation (mm)**: Precipitation affects the amount of water vapor in the atmosphere, directly impacting refractivity. Higher precipitation increases humidity, which generally leads to an increase in refractivity values due to the presence of more moisture in the air (Guerra & Garcia, 2020).

These predictors were derived from the ERA5 reanalysis dataset and were essential in training the machine learning models used to predict surface refractivity across different climatic zones.

3.3 Machine Learning Models: Three machine learning models were employed to predict surface refractivity based on atmospheric predictors such as variables like potential evaporation, surface net solar radiation, wind speed, and precipitation.

- **LightGBM**: A gradient boosting framework known for its fast-training speed and efficiency in handling large datasets. It builds decision trees in a sequential manner, optimizing for performance through boosting.
- **Random Forest**: An ensemble learning method that builds multiple decision trees and aggregates their outputs to improve prediction accuracy. Random Forest is particularly robust to overfitting and handles nonlinear relationships well.
- **LSTM (Long Short-Term Memory)**: A type of recurrent neural network (RNN) architecture designed to capture sequential dependencies in data. LSTM is well-suited

for time-series forecasting, making it ideal for modelling refractivity over time as it accounts for historical atmospheric trends.

3.3.1 Model Training and Optimization: To optimize model performance, hyperparameter tuning was conducted using grid search, a method proven effective in machine learning studies (Bergstra et al., 2011). A range of parameters was explored:

- **LightGBM**: Learning rate, number of boosting iterations, and maximum tree depth.
- **Random Forest**: Number of trees, maximum depth, and minimum samples split.
- **LSTM**: Number of hidden layers, number of LSTM units, learning rate, and sequence length.

Early stopping was applied during model training to prevent overfitting by halting training once the model's performance stopped improving on validation data. Cross-validation was also employed to ensure that the models generalized well to unseen data.

The models were trained and validated on 80% of the dataset, while the remaining 20% was used for testing. To evaluate model performance across different locations and seasons, the dataset was stratified based on these variables during the splitting process.

3.4 Evaluation Metrics: The performance of the machine learning models was assessed using the following metrics:

- **Mean Absolute Error (MAE)**: Measures the average magnitude of the errors between predicted and actual values, providing a simple interpretation of model accuracy.
- **Root Mean Square Error (RMSE)**: A more sensitive metric to large errors, highlighting significant deviations between predicted and actual refractivity.

- **R-squared (R^2)**: Indicates the proportion of variance in the actual values that is predictable from the independent variables, with higher values representing better model fit.

These metrics were computed for each location and season, enabling a comprehensive comparison of model performance across the different climatic zones. **Box plots** and **error distributions** were used to visualize the error spread across different locations and models, providing insights into model robustness and generalization across varying atmospheric conditions.

4. RESULTS AND DISCUSSION

The analysis of machine learning models (LightGBM, Random Forest, and LSTM) for predicting surface radio refractivity across five diverse climatic zones as shown in ***figure 1*** for West Africa, using atmospheric data, yielded insightful findings regarding model performance and the influence of atmospheric parameters. Key metrics like Mean Squared Error (MSE) and Mean Absolute Error (MAE) were employed to evaluate the model predictions, demonstrating varying degrees of accuracy, with clear differences in performance across regions and seasons.

4.1. Model Performance Across Locations and Climatic Zones: The comparison of MSE and MAE across different locations highlights the geographical challenges faced by each model:

a. **Monrovia**: LightGBM and Random Forest tended to overestimate refractivity, with predicted values above actual measurements. LSTM provided closer estimates but still **underestimated** refractivity by a significant margin.

b. **Niamey**: All models struggled to accurately predict refractivity in this region, with Random Forest showing slightly better accuracy. This suggests that additional

meteorological factors not fully captured by the models may be at play, such as localized temperature or pressure fluctuations.

c. **Jos**: LSTM was the most accurate in this region, reflecting its ability to capture sequential dependencies in the data, while LightGBM and Random Forest underestimated refractivity due to the complex topographical effects of this region.

d. **Dakar**: All models exhibited significant challenges here, with consistent underestimation of refractivity, indicating the need for more robust data on oceanic influences and humidity to improve model performance.

e. **Bamako (Semi-Arid zone):** LightGBM performed relatively well, but all models showed higher errors compared to other regions, likely due to the semi-arid conditions and fluctuating humidity levels. Random Forest struggled the most, suggesting that models might need to incorporate additional predictors for arid regions.

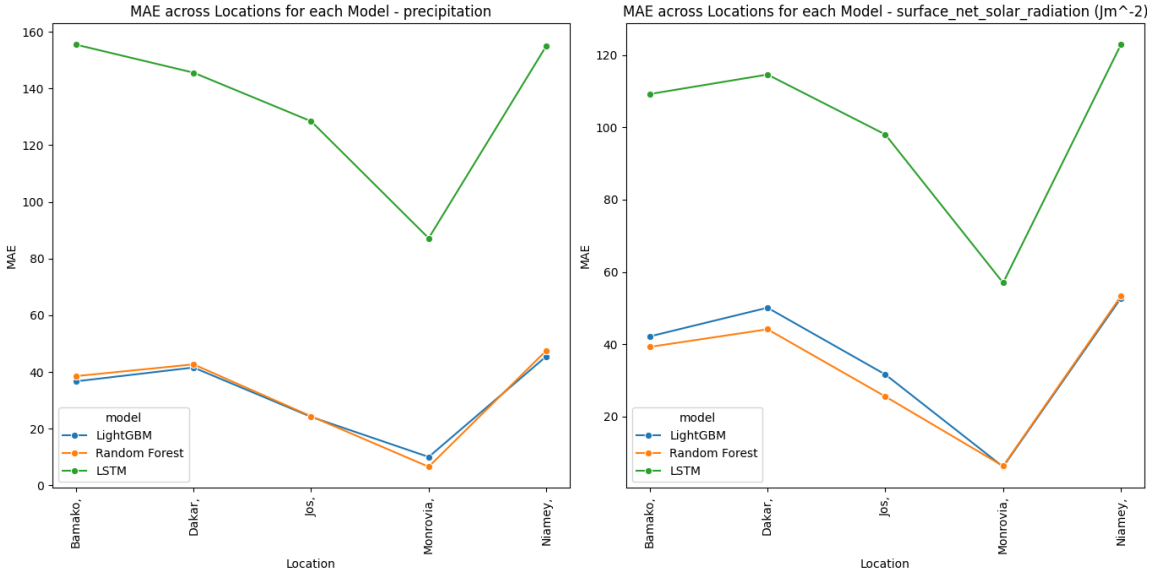

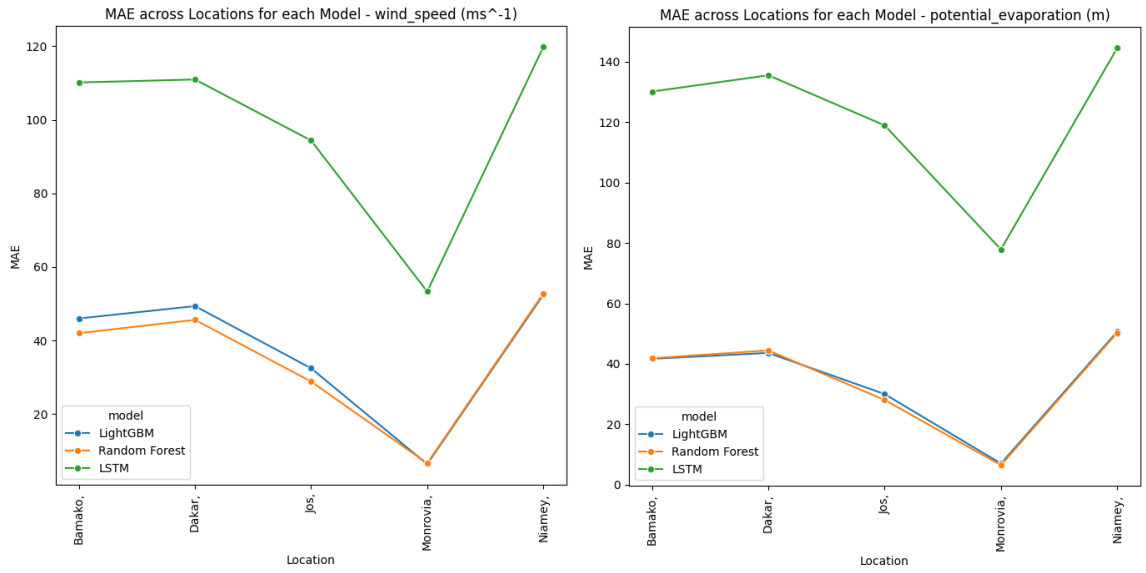

Figure 2. Mean Absolute Error (MAE) and Mean Squared Error (MSE) comparisons across locations for LightGBM, Random Forest, and LSTM models

The results, as depicted in the figure depicting ***MAE and MSE across Locations*** and the figure 3 showing the ***box plot***, show that ***LightGBM consistently performed better across most locations***, particularly in Niamey (Tropical Savannah) and Bamako (Hot Semi-Arid), regions characterized by relatively stable atmospheric conditions. LightGBM's ability to handle large datasets and efficiently learn from them enabled it to capture the relationships between atmospheric parameters and surface refractivity more effectively. In contrast, ***Random Forest*** struggled with the higher variability in data from complex climatic regions, such as Monrovia (Tropical Rainforest), where humidity and temperature fluctuations are more pronounced.

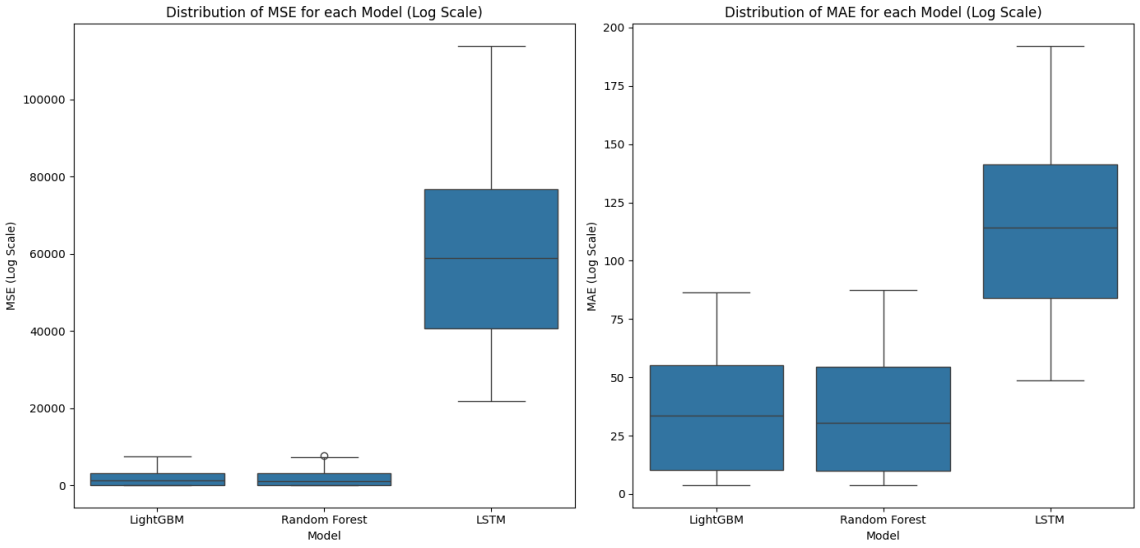

Figure 3. Box plot visualizing the error distributions (MSE and MAE) for LightGBM, Random Forest, and LSTM across different locations

Figure 2 shows the **MSE and MAE across locations** for each model, with **LightGBM** consistently outperforming the others in **Niamey** and **Bamako**. In contrast, **Figure 3** illustrates the **box plot** for error distributions, where **LSTM** shows a marked improvement in regions with seasonal variability, such as **Monrovia** and **Dakar**. However, ***LSTM's overall predictive accuracy was slightly lower*** than LightGBM due to the complexity and variability in training this type of model, particularly in handling non-stationary data without large-scale temporal patterns.

4.2. Seasonal Variation and Model Response: The ***MSE and MAE across Months*** chart in figure 4, highlights significant seasonal variation in model performance, particularly during the rainy season, when atmospheric parameters such as humidity and temperature fluctuate rapidly. During the dry season, when atmospheric conditions are more stable, all models demonstrated improved accuracy, though LightGBM maintained the lowest error rates overall. During the rainy season, ***LSTM showed improvements***, likely due to its

ability to process sequential data and capture short-term temporal dependencies. However, ***Random Forest exhibited the most significant drop in performance*** during periods of high variability, likely due to its inherent inability to manage the non-linearities in rapidly changing atmospheric conditions as effectively as LightGBM and LSTM.

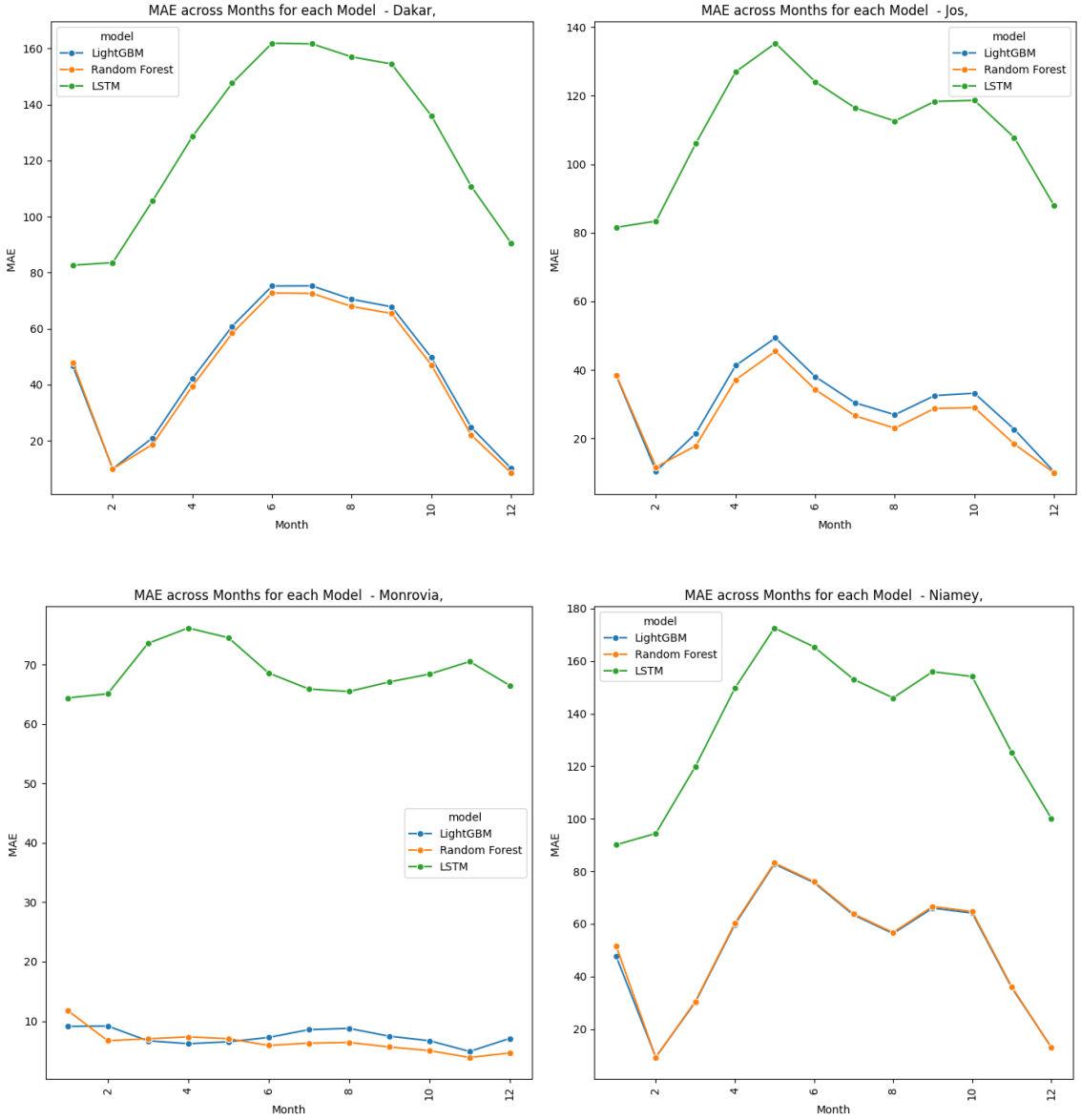

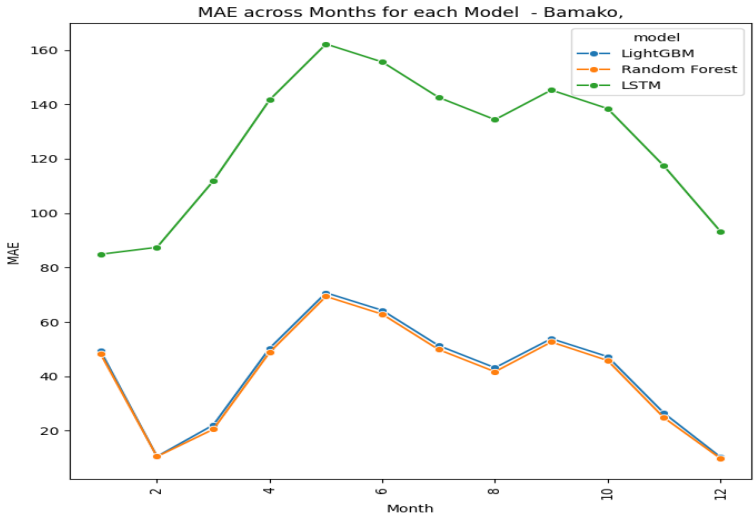

Figure 4. Mean Absolute Error (MAE) comparisons for each location across different months, showing seasonal variation in model performance

4.3. Importance of Predictors: Figure 5 uses a ***heatmap to depict the correlation between atmospheric predictors and model outputs***. This ***heatmaps*** of normalized Mean Squared Error (MSE) and Mean Absolute Error (MAE) reveal the significance of atmospheric predictors in refractivity modeling. ***Precipitation*** and ***potential evaporation*** emerge as the most impactful variables, particularly for the LSTM model, which exhibits the highest error rates for these predictors. This suggests that LSTM struggles to capture the rapid variability associated with these factors. In contrast, ***LightGBM and Random Forest*** models show significantly lower errors (MSE: ~0.02), demonstrating superior performance in managing these parameters. Whereas, when ranking across board as shown in ***table 2***, the atmospheric parameters, ***wind speed*** emerges as the most influential or stable predictor, with the lowest average errors, followed closely by ***surface net solar radiation***. Surprisingly, precipitation, despite its high MSE and MAE values in the **LSTM model**, ranked as the least significant predictor across all models. This outcome likely arises from the **high temporal and spatial variability** of precipitation, which introduces greater noise into the prediction models.

Precipitation's non-linear relationship with refractivity, combined with rapid changes during wet seasons, can challenge models like LSTM, which depend on sequential patterns. In contrast, more stable predictors, such as **wind speed** and **solar radiation**, contribute to better model performance due to their relatively **steady and predictable influence** on atmospheric refractivity. ***Potential evaporation*** ranks third, with moderate MSE and MAE scores, indicating its intermediate role in refractivity changes.

Table 2: Atmospheric Parameter Ranking Table

Atmospheric Parameter	MSE Mean	MAE Mean	MSE Rank	MAE Rank
Windspeed	17990.018	56.738	1	1
Surface Net Solar Radiation	18440.322	56.855	2	2
Potential Evaporation	22744.379	63.417	3	3
Precipitation	25427.392	65.960	4	4

Overall, ***Surface net solar radiation*** and ***wind speed*** contribute moderately to model performance. LSTM has higher error rates, indicating difficulty in capturing the temporal influence of these factors, whereas ***LightGBM and Random Forest*** maintain low error levels across all predictors.

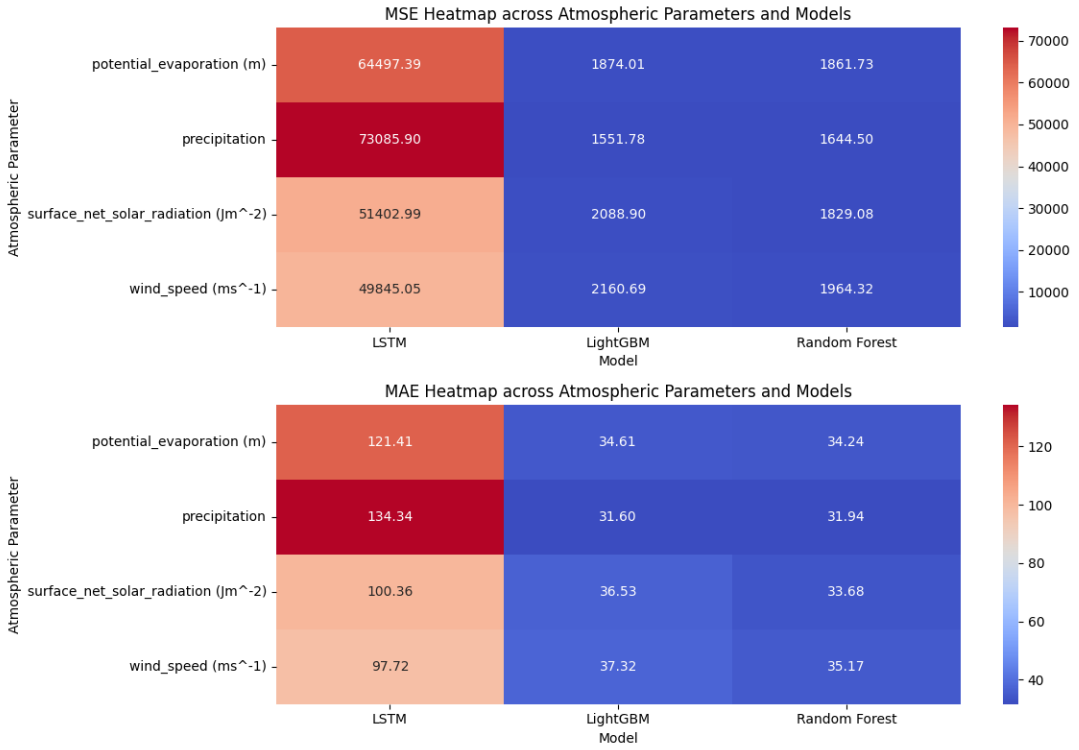

Figure 5. Heatmap illustrating the correlation between atmospheric predictors (e.g., wind speed) and model performance (LightGBM, Random Forest, LSTM)

4.4. Model Comparison and Implications: The box plot in ***figure 3*** comparing MSE and MAE across models highlights LightGBM's superior performance in minimizing errors, followed closely by Random Forest, with LSTM trailing behind.

The overall ranking of the models, shown in Table 3, indicates that **Random Forest** had the lowest MSE and MAE overall, performing particularly well in **regions with moderate climatic variability**, such as **Niamey** and **Bamako**. However, **LightGBM** emerged as the most reliable model across **diverse climatic zones**, especially in areas with extreme weather conditions, where its robustness in handling large, complex datasets gave it an edge. This makes LightGBM the more consistent model for broader applications, while Random Forest shows strong performance in more stable conditions. This is likely due to its gradient boosting framework, which excels in handling structured datasets with various

interdependencies between predictors. ***LSTM*** performed well in regions and seasons where temporal patterns were more pronounced, suggesting that its sequential architecture may be more appropriate for specific use cases involving highly seasonal or time-dependent refractivity predictions.

Table 3: Model Ranking

Model	MSE Mean	MAE Mean	MSE Rank	MAE Rank
Random Forest	1824.906	33.757	1	1
LightGBM	1918.844	35.014	2	2
LSTM	59707.833	113.457	3	3

4.5. Implications for Radio Refractivity Prediction and Wireless Communication Systems: This study's findings have important implications for enhancing radio refractivity predictions, particularly in West Africa's diverse climatic zones. Accurate refractivity predictions are crucial for optimizing wireless communication systems, minimizing signal degradation, and improving network reliability.

- **Tropical and Coastal Zones**: The high variability of atmospheric conditions, particularly due to humidity and oceanic influences, suggests that more complex models or additional predictors may be needed to accurately capture these fluctuations. LightGBM performs well, but enhancements through sequential data or additional humidity-related predictors could improve accuracy.
- **Highland and Semi-Arid Zones**: Models that incorporate sequential data, like **LSTM**, may be better suited for highland and semi-arid zones, where temporal variations in wind speed and solar radiation are key refractivity drivers. While LSTM

underperformed overall, its potential for handling time-dependent data makes it valuable in these specific zones.

- **Practical Implications**:

LightGBM's superior performance highlights its potential for improving network reliability and reducing signal degradation across West Africa. By providing more accurate refractivity predictions, telecommunication companies can better anticipate signal disruptions during extreme weather conditions, particularly in **coastal regions** like **Dakar** where oceanic influences and high humidity impact signal strength. Furthermore, the deployment of machine learning models like **LightGBM** could **reduce operational costs** by enabling more efficient **network designs** that account for atmospheric variability, leading to enhanced **service quality** in rural and high-demand urban areas, making it a viable model for deployment in communication systems across the region.

5. CONCLUSION

This study demonstrates the potential of machine learning models for predicting surface refractivity in West Africa. Among the models tested, **LightGBM** consistently delivered the most accurate predictions, particularly in arid and semi-arid regions. **LSTM** showed promise in areas with high seasonal variability, while Random Forest performed well but lagged behind in overall predictive accuracy.

Key findings indicate that:

- **LightGBM** is the most reliable model for surface refractivity predictions, especially in less extreme climatic conditions.
- **LSTM** has potential for regions with significant seasonal changes due to its ability to handle sequential data.

- **Random Forest** showed strong performance but exhibited a higher tendency toward overfitting.

These results suggest promising future directions for enhancing refractivity predictions. Potential improvements could include integrating additional atmospheric predictors, real-time data, and using hybrid or ensemble models that combine the strengths of LightGBM and LSTM for regions with complex climate patterns. Fine-tuning model hyperparameters for specific climatic zones could further improve accuracy.

In summary, **LightGBM** stands out as the most promising model for refractivity prediction in West Africa, offering significant improvements over traditional methods.

REFERENCES

Bergstra, J., Bardenet, R., Bengio, Y., & Kégl, B. (2011). Algorithms for hyper-parameter optimization. **Advances in Neural Information Processing Systems, 24**, 2546-2554.

Bouma, H., Hermans, L., Van Der Loo, S., & De Bruin, S. (2021). Machine learning for global climate model prediction: Evaluating the performance of a random forest. **Climate Dynamics, 57**(5-6), 1669-1685. https://doi.org/10.1007/s00382-020-05460-w

Breiman, L. (2001). Random forests. **Machine Learning, 45**(1), 5-32. https://doi.org/10.1023/A:1010933404324

Dee, D. P., Uppala, S. M., Simmons, A. J., et al. (2011). The ERA-Interim reanalysis: Configuration and performance of the data assimilation system. **Quarterly Journal of the Royal Meteorological Society, 137**(656), 553-597. https://doi.org/10.1002/qj.828

ECMWF. (2020). ERA5 reanalysis dataset. **European Centre for Medium-Range Weather Forecasts**. https://www.ecmwf.int/en/forecasts/datasets/reanalysis-datasets/era5

Gentine, P., Park, S., Ryu, Y., et al. (2018). Machine learning for land surface evaporation: Algorithms, methods, and the challenges ahead. **Water Resources Research, 54**(9), 6794-6811. https://doi.org/10.1029/2018WR022616

Guerra, E., & Garcia, J. (2020). A machine learning approach to predict rain-induced attenuation in wireless networks. **IEEE Access, 8**, 128917-128927. https://doi.org/10.1109/ACCESS.2020.3008767

Hochreiter, S., & Schmidhuber, J. (1997). Long short-term memory. **Neural Computation, 9**(8), 1735-1780. https://doi.org/10.1162/neco.1997.9.8.1735

Kalansuriya, C., Gunawardena, S., & Wijekoon, P. (2015). Application of machine learning techniques for atmospheric refractivity prediction. **Journal of Atmospheric Science**.

Ke, G., Meng, Q., Finley, T., Wang, T., Chen, W., Ma, W., Ye, Q., & Liu, T. Y. (2017). LightGBM: A highly efficient gradient boosting decision tree. **Advances in Neural Information Processing Systems, 30**, 3146-3154. https://papers.nips.cc/paper/6907-lightgbm-a-highly-efficient-gradient-boosting-decision-tree

Liaw, A., & Wiener, M. (2002). Classification and regression by Random Forest. **R News, 2**(3), 18-22. https://CRAN.R-project.org/doc/Rnews/

Tang, Y., & Lin, H. (2020). Application of LSTM in meteorological time-series prediction. **International Journal of Forecasting, 36**(3), 1261-1270. https://doi.org/10.1016/j.ijforecast.2019.11.002

Thies, B., & Bendix, J. (2011). Satellite-based rainfall detection: Assessment of the performance of the machine learning methods. **Journal of Hydrometeorology, 12**(6), 1478-1490. https://doi.org/10.1175/2011JHM1344.1

Wilby, R. L., & Dawson, C. W. (2013). The statistical downscaling model: Insights from one decade of application. **International Journal of Climatology, 33**(7), 1707-1719. https://doi.org/10.1002/joc.3544

APPENDIX

The following appendix provides detailed comparisons of model performance and predictions, supplementing the findings discussed in the main text. These results offer further insights into model accuracy across different climatic zones and over time.

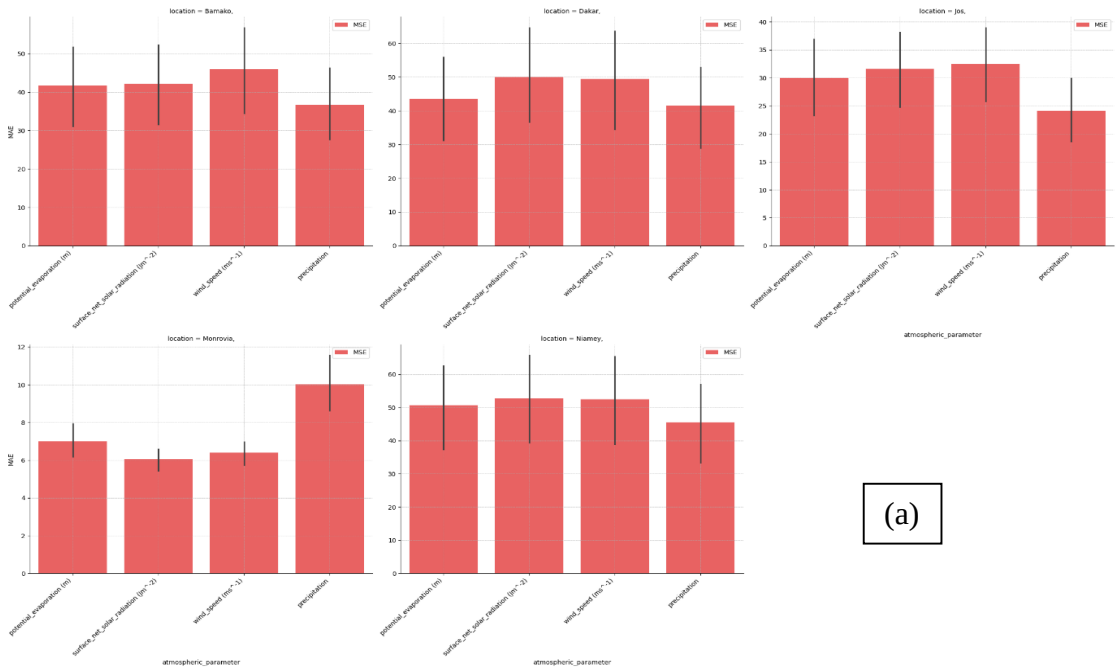

(a)

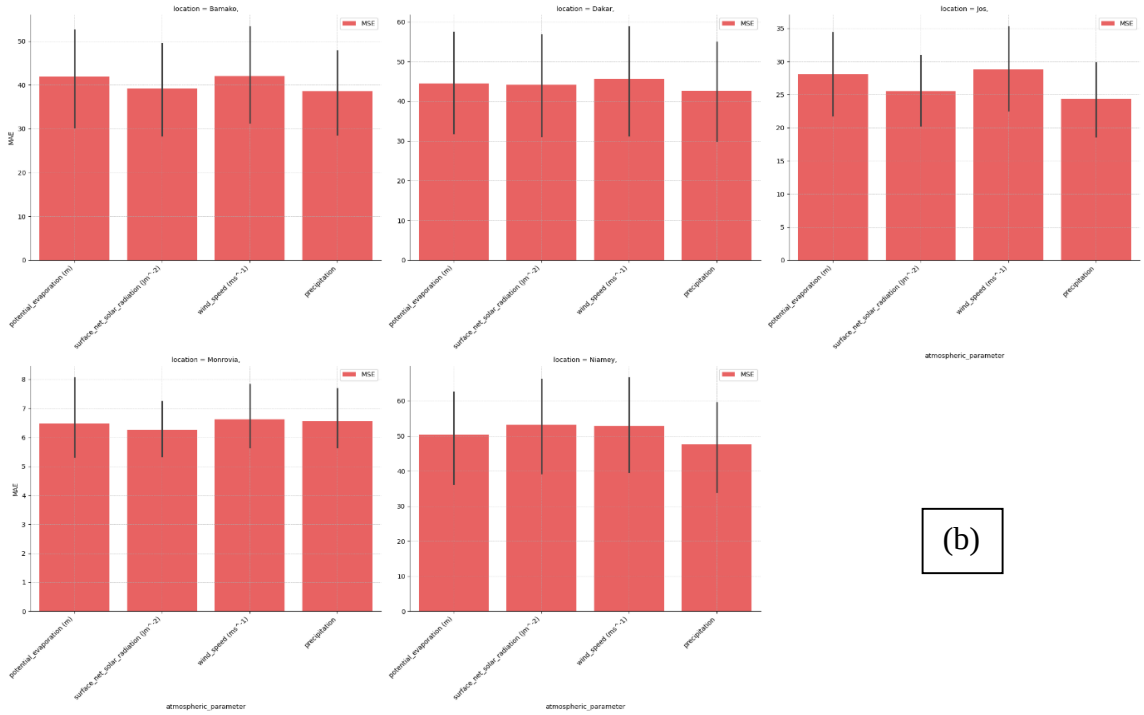

(b)

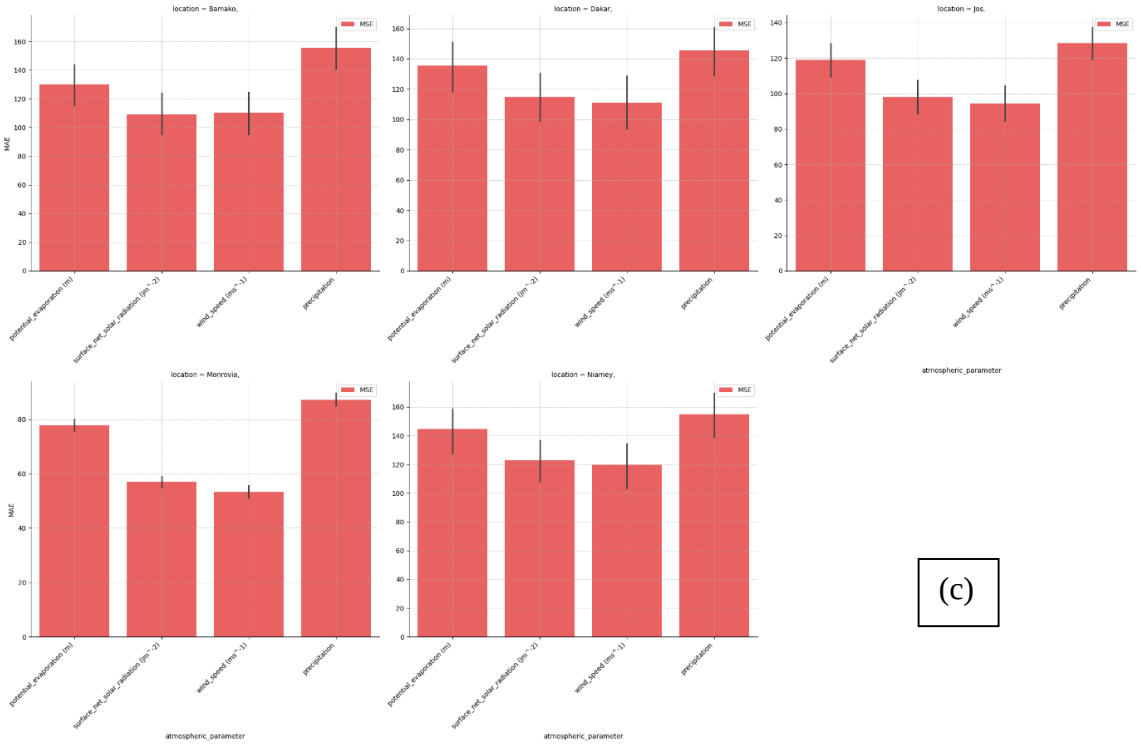

(c)

Appendix Figure 1: Model Performance with respect to each predictor (a) LightGBM (b) RandomForest (c) LSTM

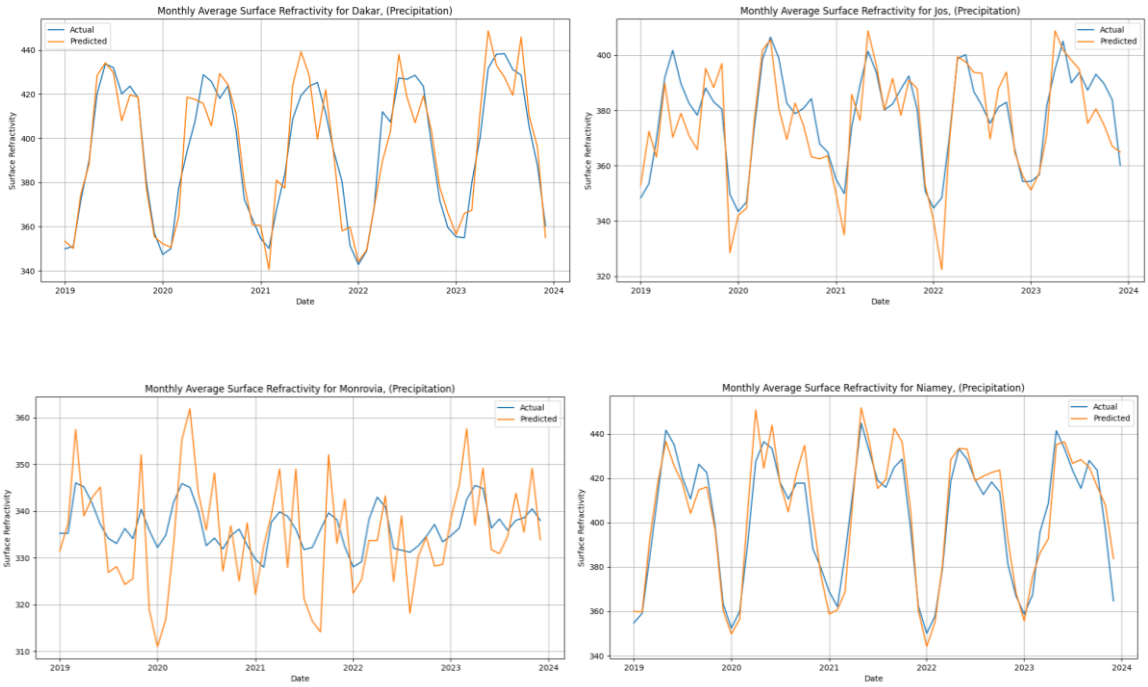

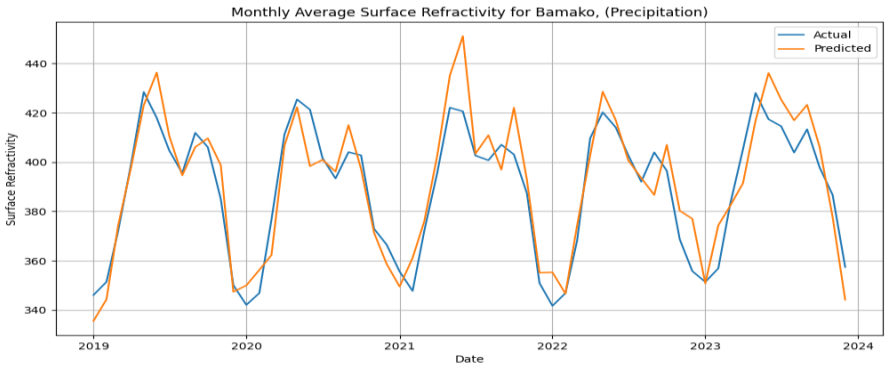

Appendix Figure 2: LightGBM Prediction vs Actual values

Appendix Table 1: Table Showing LightGBM Prediction vs Actual values

YEAR	SURFACE REFRACTIVITY	PREDICTED SURF	LOCATION	ZONE
2019	337.8905	335.7131	Monrovia,	Tropical Rainforest
2020	336.8705	336.1424	Monrovia,	Tropical Rainforest
2021	335.0587	333.2645	Monrovia,	Tropical Rainforest
2022	334.3544	330.2382	Monrovia,	Tropical Rainforest
2023	339.1473	340.562	Monrovia,	Tropical Rainforest
2019	402.6694	400.3903	Niamey,	Tropical Savannah
2020	402.7075	407.3609	Niamey,	Tropical Savannah
2021	404.9511	405.8499	Niamey,	Tropical Savannah
2022	398.5185	402.0268	Niamey,	Tropical Savannah
2023	404.9335	405.9945	Niamey,	Tropical Savannah
2019	389.2038	390.0405	Bamako,	Hot Semi-Arid
2020	388.7995	386.3005	Bamako,	Hot Semi-Arid
2021	388.9961	396.5275	Bamako,	Hot Semi-Arid
2022	385.1957	389.4236	Bamako,	Hot Semi-Arid
2023	393.0877	395.4774	Bamako,	Hot Semi-Arid
2019	395.9212	395.053	Dakar,	Coastal
2020	392.829	394.2528	Dakar,	Coastal
2021	389.4156	390.6169	Dakar,	Coastal
2022	393.081	390.6349	Dakar,	Coastal
2023	401.2491	403.2687	Dakar,	Coastal
2019	376.4732	372.5792	Jos,	Highland
2020	377.3313	372.3295	Jos,	Highland
2021	378.2501	378.1415	Jos,	Highland
2022	374.3321	374.2502	Jos,	Highland
2023	382.6947	378.9572	Jos,	Highland

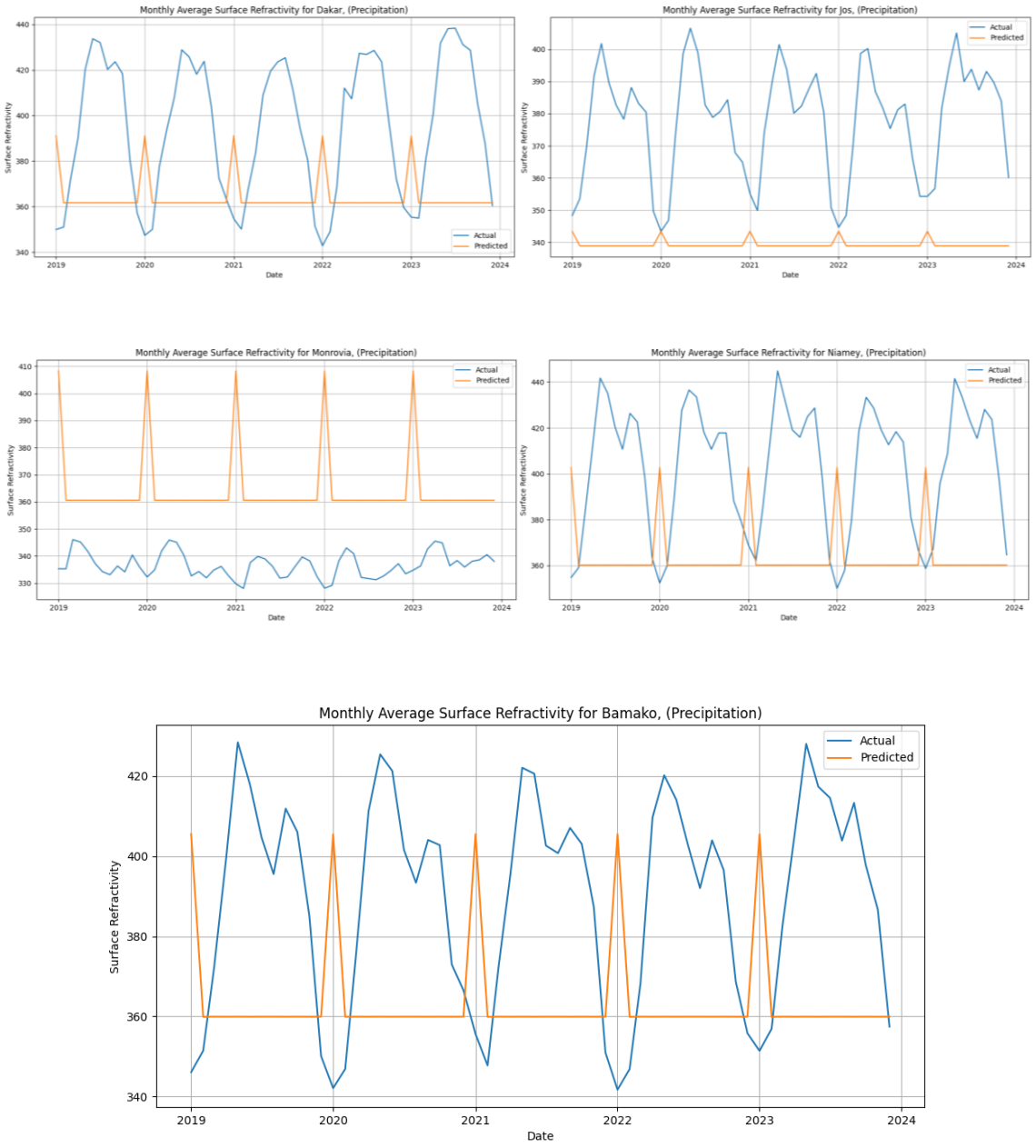

Appendix Figure 3: Random Forest Prediction vs Actual values

Appendix Table 2: Table Showing RandomForest Prediction vs Actual values

YEAR	SURFACE REFRACTIVITY	PREDICTED SURF	LOCATION	ZONE
2019	337.8905	364.6313	Monrovia,	Tropical Rainforest
2020	336.8705	364.6207	Monrovia,	Tropical Rainforest
2021	335.0587	364.6313	Monrovia,	Tropical Rainforest
2022	334.3544	364.6313	Monrovia,	Tropical Rainforest
2023	339.1473	364.6313	Monrovia,	Tropical Rainforest
2019	402.6694	363.8152	Niamey,	Tropical Savannah
2020	402.7075	363.8066	Niamey,	Tropical Savannah
2021	404.9511	363.8152	Niamey,	Tropical Savannah
2022	398.5185	363.8152	Niamey,	Tropical Savannah
2023	404.9335	363.8152	Niamey,	Tropical Savannah
2019	389.2038	363.791	Bamako,	Hot Semi-Arid
2020	388.7995	363.7817	Bamako,	Hot Semi-Arid
2021	388.9961	363.791	Bamako,	Hot Semi-Arid
2022	385.1957	363.791	Bamako,	Hot Semi-Arid
2023	393.0877	363.791	Bamako,	Hot Semi-Arid
2019	395.9212	364.1814	Dakar,	Coastal
2020	392.829	364.176	Dakar,	Coastal
2021	389.4156	364.1814	Dakar,	Coastal
2022	393.081	364.1814	Dakar,	Coastal
2023	401.2491	364.1814	Dakar,	Coastal
2019	376.4732	339.2992	Jos,	Highland
2020	377.3313	339.2983	Jos,	Highland
2021	378.2501	339.2992	Jos,	Highland
2022	374.3321	339.2992	Jos,	Highland
2023	382.6947	339.2992	Jos,	Highland

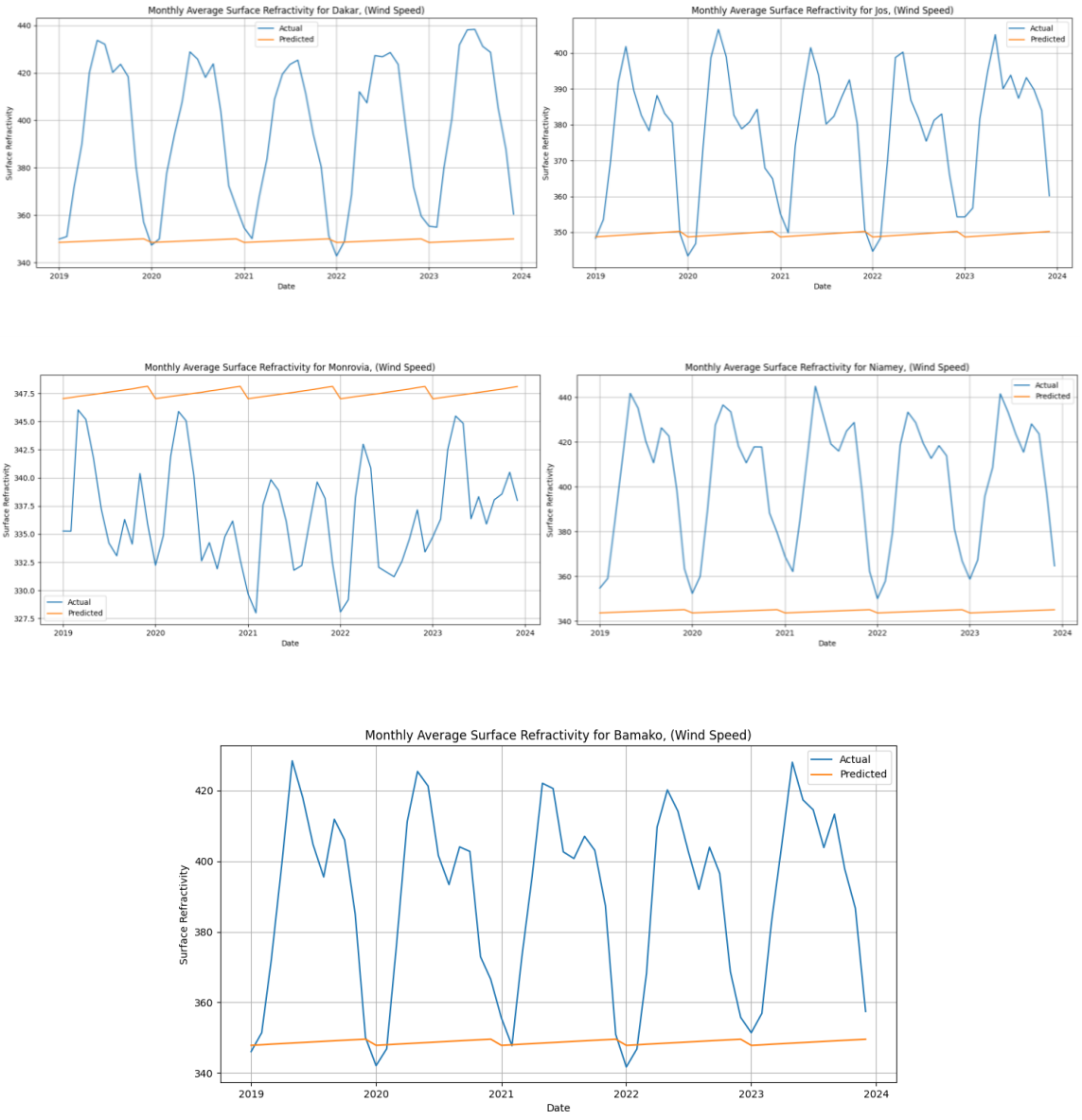

Appendix Figure 4: LSTM Prediction vs Actual values

Appendix Table 3: Table Showing LSTM Prediction vs Actual values

YEAR	SURFACE REFRACTIVITY	PREDICTED SURF	LOCATION	ZONE
2019	337.8905	347.5713	Monrovia,	Tropical Rainforest
2020	336.8705	347.5685	Monrovia,	Tropical Rainforest
2021	335.0587	347.5628	Monrovia,	Tropical Rainforest
2022	334.3544	347.5555	Monrovia,	Tropical Rainforest
2023	339.1473	347.5492	Monrovia,	Tropical Rainforest
2019	402.6694	344.4465	Niamey,	Tropical Savannah
2020	402.7075	344.4373	Niamey,	Tropical Savannah
2021	404.9511	344.4315	Niamey,	Tropical Savannah
2022	398.5185	344.4238	Niamey,	Tropical Savannah
2023	404.9335	344.4161	Niamey,	Tropical Savannah
2019	389.2038	348.7311	Bamako,	Hot Semi-Arid
2020	388.7995	348.7225	Bamako,	Hot Semi-Arid
2021	388.9961	348.7174	Bamako,	Hot Semi-Arid
2022	385.1957	348.7104	Bamako,	Hot Semi-Arid
2023	393.0877	348.7036	Bamako,	Hot Semi-Arid
2019	395.9212	349.2865	Dakar,	Coastal
2020	392.829	349.2761	Dakar,	Coastal
2021	389.4156	349.2694	Dakar,	Coastal
2022	393.081	349.2608	Dakar,	Coastal
2023	401.2491	349.2522	Dakar,	Coastal
2019	376.4732	349.4831	Jos,	Highland
2020	377.3313	349.4727	Jos,	Highland
2021	378.2501	349.4655	Jos,	Highland
2022	374.3321	349.4564	Jos,	Highland
2023	382.6947	349.4475	Jos,	Highland